Integrated Approach for the Safety Evaluation of Masonry Bridges

Valerio Sabbatini, Silvia Santini, Claudio Sebastiani and
Eugenio Ricci

May 12, 2024

CODE 308

INTEGRATED APPROACH FOR THE SAFETY EVALUATION OF MASONRY BRIDGES

KEYWORDS: Masonry Bridges, Unmanned Aerial Vehicle (UAV), Building Information Model (BIM), Finite Element Model (FEM), Nonlinear Static Analysis

ABSTRACT

Infrastructure is the backbone for the economic and social development of a territory, influencing its productivity, facilitating trade with other areas and markets, improving economic and social inclusion, and ensuring its environmental and climate sustainability.

Italy has a rich and diverse asset of transport infrastructures. After the collapse of the Viadotto Polcevera in Genoa in 2018, the Italian Ministry of Infrastructure and Transportation enacted an important and extended plan for a united safety management of bridges.

In this scenario, masonry bridges represent a particular type of infrastructure due to their dated design and the employment of heterogenous materials. In this work, it is presented an integrated approach for the safety evaluation of masonry bridges which combines the use of Unmanned Aerial Vehicle (UAV) and testing. The collected data is processed and employed with the Building Information Model (BIM) working methodology to define the digital twin of the bridge. The BIM model is used to organize the collected information and set the finite element model (FEM) of the bridge. Finally, nonlinear static analyses are adopted to evaluate the safety coefficients of the structures under traffic loads.

The approach represents a comprehensive workflow to integrate modern technologies and methodologies as UAV, BIM, and nonlinear analysis to improve the safety evaluation of masonry infrastructures.

1. INTRODUCTION

Infrastructure is the backbone for the economic and social development of a territory, and bridges represent one of the most critical parts of the infrastructure system. Safety and serviceability are crucial aspects for the infrastructure management, thus the necessity to define and validate robust procedures for structural assessment which efficiently integrates survey, diagnostic and modelling. For masonry bridges, the irregular geometries, and the reduced knowledge on the mechanical properties of the materials are critical factors. The most recent masonry bridge was built about a century ago however a significant amount of these structures is still in use today. At the beginning of the twentieth century, the masonry bridge was progressively abandoned but the existing structures were kept in service and in some cases updated with reinforced concrete strengthening interventions.

In this context, modelling is a central activity for the evaluation of the capacity of the structure. Solla et al. [1] proposed a modelling approach based on photogrammetry and ground-penetrating radar to retrieve a complete representation of the internal and external geometry of a masonry stone bridge. Domede et al. [2] presented a structural analysis technique based on an orthotropic damage model combining historical research and laboratory tests on core samples. Borlenghi et al. [3] carried out an extensive research to assess the structural conditions of the historic bridge of Olla comprehensive of historical research, geomatic survey, on-site visual inspection, limited local tests on materials, operational modal testing and analysis, and finite element model with the choice of the uncertain structural parameters and identification of the optimal parameters.

In this research a multidisciplinary assessment approach is applied to a masonry viaduct on the Limentra river built in the beginning of the 1900 in the province of Pistoia in Tuscany (Italy). Multidisciplinary activities were performed: historical-critical analysis on the evolution of the bridge as partial reconstructions and past strengthening interventions; the external geometry was retrieved from drone photogrammetry; the structural details and the internal morphology of the structure was retrieved from in-situ testing and interpretation of the structural drawings; the information was merged in the Building Information Model (BIM), and the structural model based on the finite element method was employed to carry out non-linear static analysis under traffic loads. The research highlights the potentials of integrating multidisciplinary data in the structural assessment of masonry bridges. The adopted approach was employed to assess the capacity of the structure in its operational conditions.

2 THE CASE STUDY: THE LIMENTRA BRIDGE

The Limentra bridge is a multi-span masonry viaduct located in the province of Pistoia, Tuscany (Italy) on the Province Route SP 51 (Figure 1).

Figure 1 Overview of the Limentra bridge

The bridge which crosses the Limentra river, is formed by five bays with variable spans between 10.5 and 12.9 m each and constant width of 6.70 m (Figure 2). The bridge presents three bays with full masonry arches, one bay with masonry arch strengthened by concrete intrados arch, and a reconstructed bay in reinforced concrete formed by eight pre-stressed concrete beams. The abutment of the reconstructed bay is in R.C. and the other abutment in stone masonry as the arches and piers.

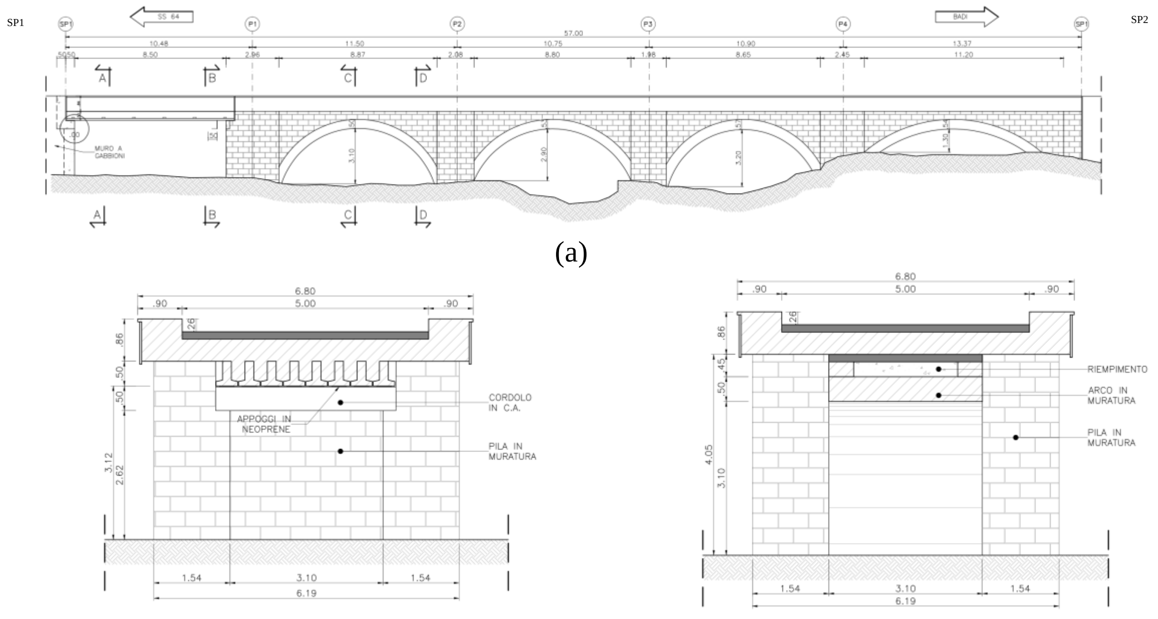

(a)

(b)

(c)

Figure 2 Technical drawings of the Limentra bridge, courtesy of Diamonds srl: (a) elevation view, (b) section B-B, (c) section C-C.

3 THE INTEGRATED APPROACH

3.1 Historical-critical analysis

The documentary research was carried out at the Archival of the Technical Office of Pistoia. According to the retrieved information, the first (SP1-P1) and the last bay (P4-SP2) were originally stone masonry arches, and they collapse during the second world war (Figure 3a). The documents show the reconstruct of bay P4-SP2 by Chief Engineer P. Francese, which dates to February 1948 and reports the thickness of the concrete arch between 30 and 40 cm (Figure 3b, c).

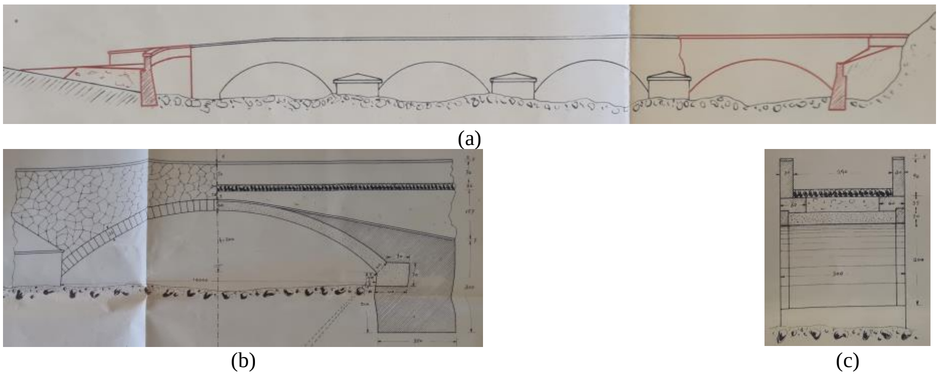

(a)

(b)

(c)

Figure 3 Archival technical drawings from the 1948 reconstruction, courtesy of the Archival of the Technical Office of Pistoia: (a) in red the collapsed elements, (b) the reconstructed bay, (c) the characteristic section of the bridge.

In March 1988, the bridge was strengthened to withstand the modern vehicle traffic. The archival documents report the pre- and post-conditions of the bridge (Figure 4a, b) along with the pictures of the site work. Six vertical and four inclined micro piles (diameter of 13 cm) were drilled into each pier. The pier section was enlarged following the base profile. The deck was enlarged and reconstructed in reinforced concrete. It is of interest that the technical drawings report the carpentry of the deck (longitudinal rebars ϕ 24 mm distanced by 15 cm, deck stirrups ϕ 10 mm distanced by 20 cm, curb stirrup ϕ 12 mm distanced by 20 cm in Figure 4c) that is different from the carpentry shown in the pictures of the site work (Figure 4d, e) for which precast concrete slab (predalles) were adopted. It is also reported bay SP1-P1 formed by eight pre-stressed concrete beams supporting the deck. A layer of polystyrene was interposed between the stone masonry arches and the new R.C. deck which substantially unloaded the arches and transferred the load to the piers.

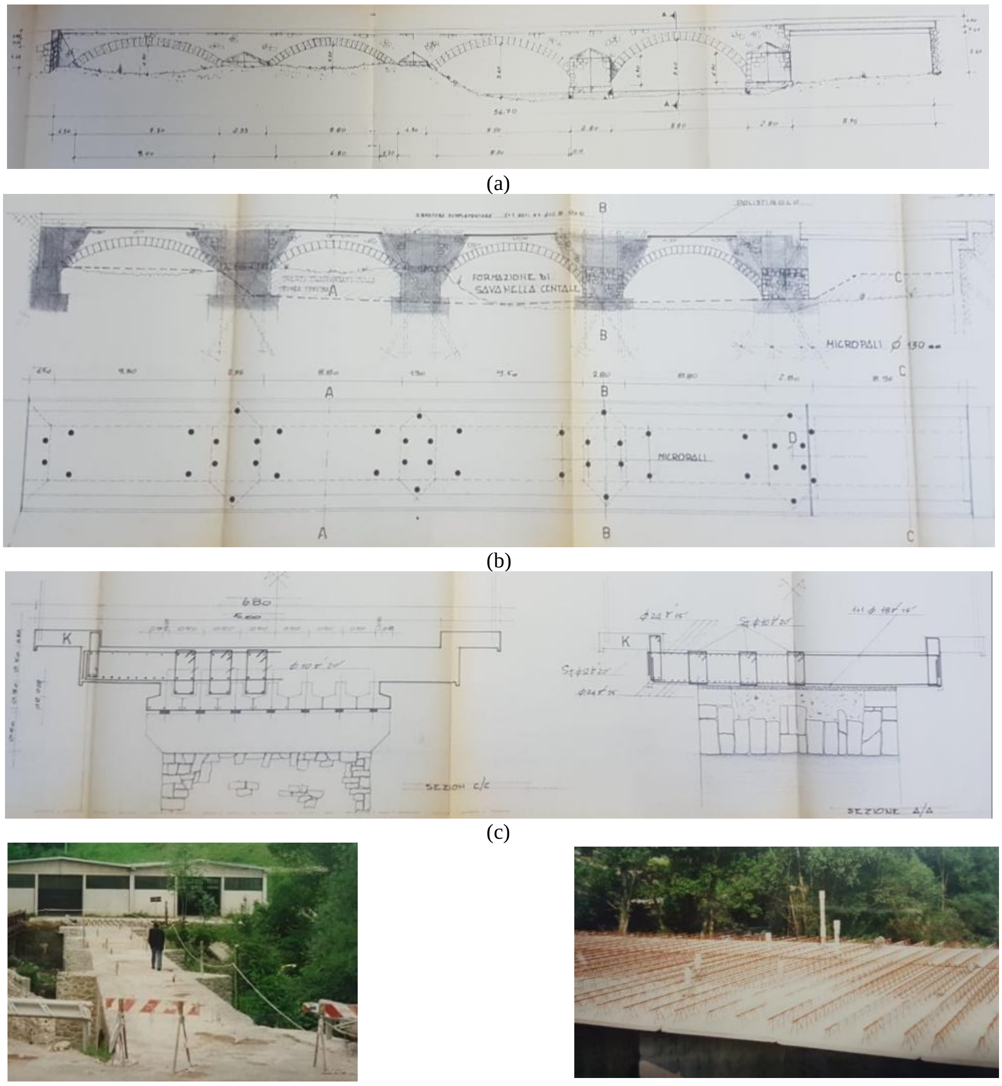

(a)

(b)

(c)

(d)

(e)

Figure 4 Archival technical drawings from the 1988 intervention, courtesy of the Archival of the Technical Office of Pistoia: (a) elevation view pre-intervention, (b) elevation view post-intervention, (c) carpentry of the transversal sections, (d) micro piles intervention on the piers, (e) precast concrete deck before the final concrete cast.

The documentary research revealed the original construction technique and the internal morphology of the bridge. The first and last bays (with longest span) underwent structural changes in 1948, although the bridge drastically changed its structural scheme with the 1988 upgrade intervention which significantly unloaded the stone masonry arches, inserted a larger reinforced concrete deck, and rigidly connected it to the piers with micro piles.

3.2 Geometrical model

In November 2022 was performed the geometrical survey of the bridge with the photogrammetric method to rely on the updated representation of the structure. The collection of data was carried out in about two hours with the use of a small Unmanned Aerial Vehicle (UAV) of 0.32 kg of weight, equipped with 21 MP camera. Twenty markers were positioned on the bridge to scale the model and facilitate the merging operations. The point cloud of the site was assembled with the software Agisoft Metashape [5] using 445 photos (Figure 5a). The data was further processed to define the three-dimensional tiled model of the bridge including the dimensional texturized surfaces that represent a fundamental reference for the identification and localization of the structural defects (Figure 5b).

(a) (b)

Figure 5 Geometrical survey of the Limentra bridge: (a) point cloud, (b) texturized tiled model.

The photogrammetric survey allowed the updated representation of the external geometry, while the internal morphology was assumed from the technical drawing and confirmed by the geo-radar survey. The information was compiled with the Building Information Model working methodology, in Figure 6a are reported the line drawings and the refined point cloud of the bridge which served for modelling in Revit [6]. A three-dimensional geometrical model of the bridge was defined respecting the four materials (stone masonry, consolidated masonry, infill and reinforced concrete as shown in Figure 6b, c, d), the material characterization retrieved from the compression test of three concrete cores was included in the object's property in BIM.

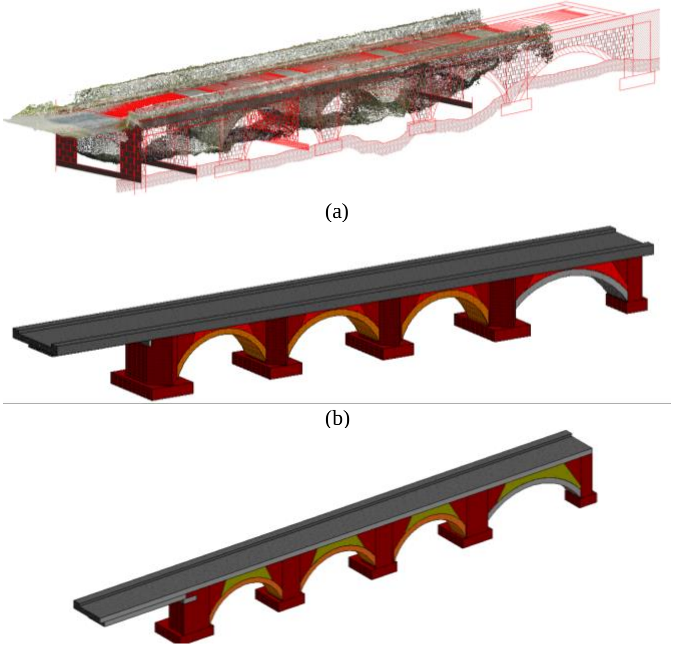

(a)

(b)

(c)

Figure 6 Modelling phases in BIM: (a) point cloud and technical line drawings reference for the geometry, (b) BIM of the Limentra bridge in grey the R.C. elements (deck and the intrados of bay SP1-P1), in dark red the consolidated stone masonry (piers), in orange and light red the original stone masonry (arches and spandrel walls), in dark yellow the backfill, (c) longitudinal section-cut of the BIM.

3.3 Structural model

The FEM of the bridge was developed in Midas FEA NX [7] using 117'000 tetrahedral elements, the model is fully constrained at the base of the foundations and horizontally constrained on the lateral surface of abutment SP2. The model was employed for the structural assessment of the piers under traffic load considering the material nonlinearity of masonry. For this purpose, the stone masonry was modelled as non-linear homogenized material based on the mechanical parameters suggested by the Italian code (table C8.5.II [8]). Being the piers consolidated with micro piles, the strengths and modulus of elasticity were increased by 40% (as suggested by the Italian code for heavy consolidation on regular stone masonry). The backfill was assumed as linear elastic homogeneous material with the weight and modulus of elasticity of an irregular soft stone masonry (according to table C8.5.II [8]).
According to the 1988 strengthening intervention, the R.C. deck was re-built and rigidly connected to the consolidated piers with nine micro piles per pier, moreover prior casting the new R.C. deck, a layer of polystyrene was interposed between the backfill and the deck. The finite element model respected these technical details by disconnecting the nodes of the finite elements of the deck from the backfill and spandrels. Therefore, the contribution of the arches, backfill, and spandrel to the stability of the piers under vertical traffic load is provided by the lateral confinement of the piers in the longitudinal direction. The adopted finite element model is reported in Figure 7.

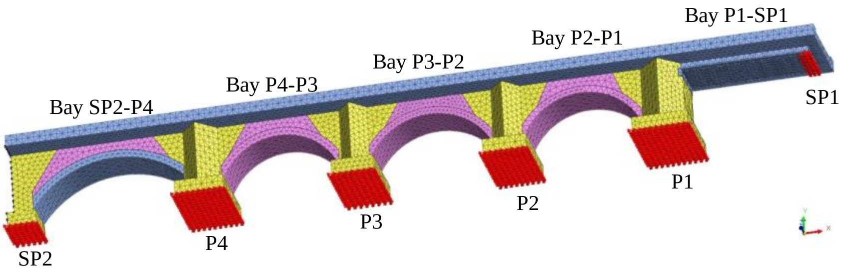

Figure 7 FEM of the bridge Limentra.

The structural model considers the material nonlinearity of the masonry with the Total Strain Crack formulation. The influence of the mesh size was accounted with the parameter h (average element dimension). The stress-strain relationship was defined as parabolic curve in compression and exponential curve in tension, the fracture energies were estimated according to Lourenço and Gaetani [9]. The adopted input parameters for the masonry are reported in Figure 8. The R.C. deck and backfill were assumed linear elastic with modulus of elasticity of 33’000 and 1080 MPa.

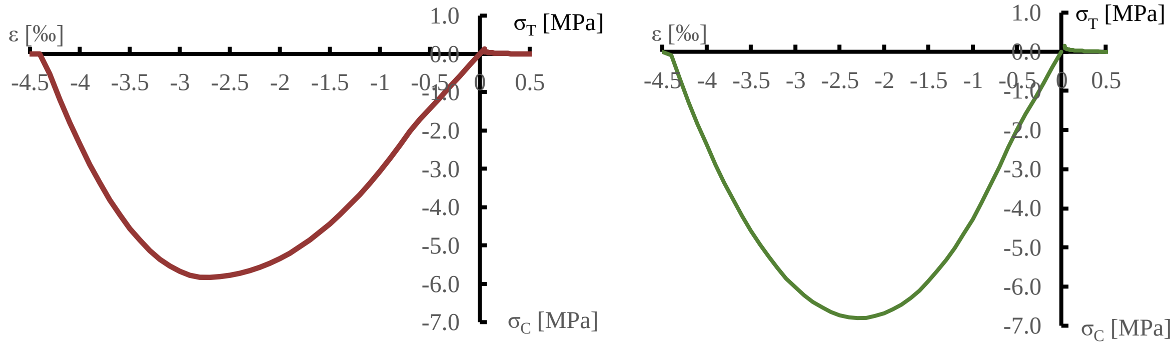

E [Mpa]	2850	G_C [N/mm]	11.789	G_T [N/mm]	0.020
f_C [Mpa]	5.833	$\varepsilon_{c, c/3}$	-0.068%		
f_T [Mpa]	0.131	$\varepsilon_{c, c}$	-0.273%	$\varepsilon_{T, c}$	0.005%
h [m]	0.184	$\varepsilon_{c, u}$	-0.438%	$\varepsilon_{T, u}$	0.042%

(a)

E [Mpa]	3990	G_c [N/mm]	14.385	G_T [N/mm]	0.028
f_C [Mpa]	8.167	$\varepsilon_{c, c/3}$	-0.057%		
f_T [Mpa]	0.184	$\varepsilon_{c, c}$	-0.227%	$\varepsilon_{T, c}$	0.005%
h [m]	0.170	$\varepsilon_{c, u}$	-0.441%	$\varepsilon_{T, u}$	0.046%

(b)

Figure 8 Nonlinear materials: (a) squared stone masonry blocks, (b) consolidated stone masonry.

The nonlinear static analysis was carried out under the vehicular traffic with scheme 1 defined in NTC2018 [4], the load configuration considers both the distributed load of 9 kN/m^2 (representing the uniform regular vehicular traffic over the two lanes), and four concentrated point loads of 150 kN each (representing the tandem load of a characteristic heavy truck on the principal lane). Eight different load configurations were analysed to maximize the effects on the four piers and the four bays. In Figure 9 are reported two exemplifying load configurations.

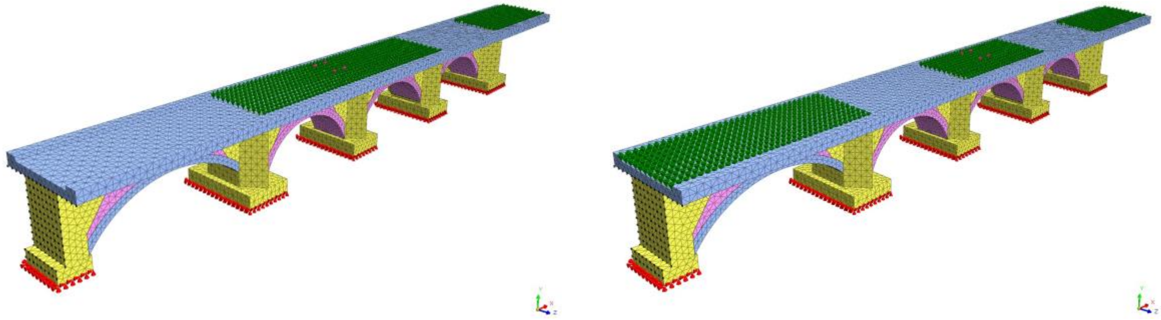

(a) (b)

Figure 9 Traffic load configurations, in green the uniformly distributed load and in pink the concentrated load: (a) combination to maximize the load effect on pier P3, (b) combination to maximize the load effect on bay P2-P3.

The nonlinear analyses were performed in two consecutive stages. In the first stage the permanent structural (G1) and non-structural (G2) loads were applied with load multipliers of 1.35. In the second stage the traffic load was monotonic incremented up to a load multiplier equal to 2. The Italian code [4] considers the structure adequate under traffic load when the vehicular traffic load multiplier reaches 1.35 (35% higher than the defined characteristic load). The results of two representative analysis are reported in Figure 10 and Figure 11.

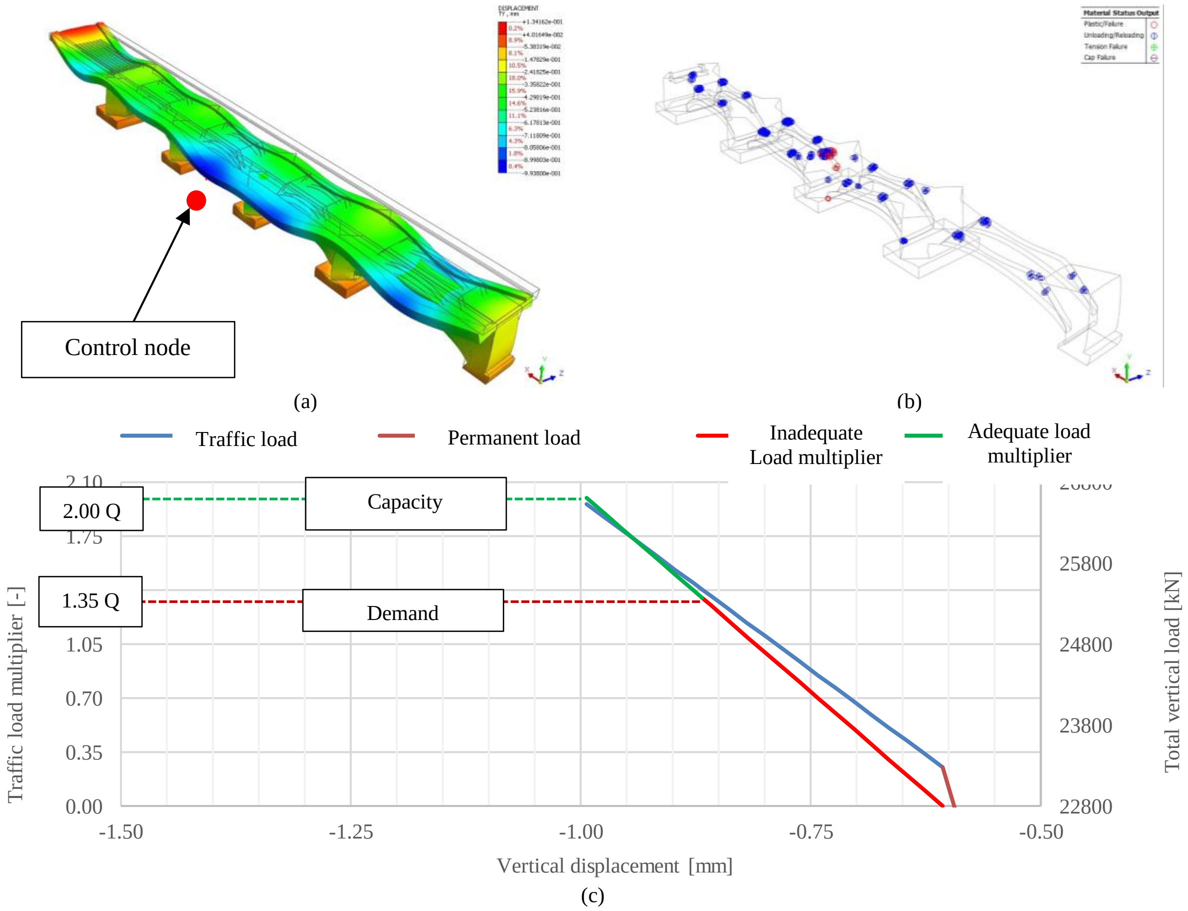

(a) (b)

(c)

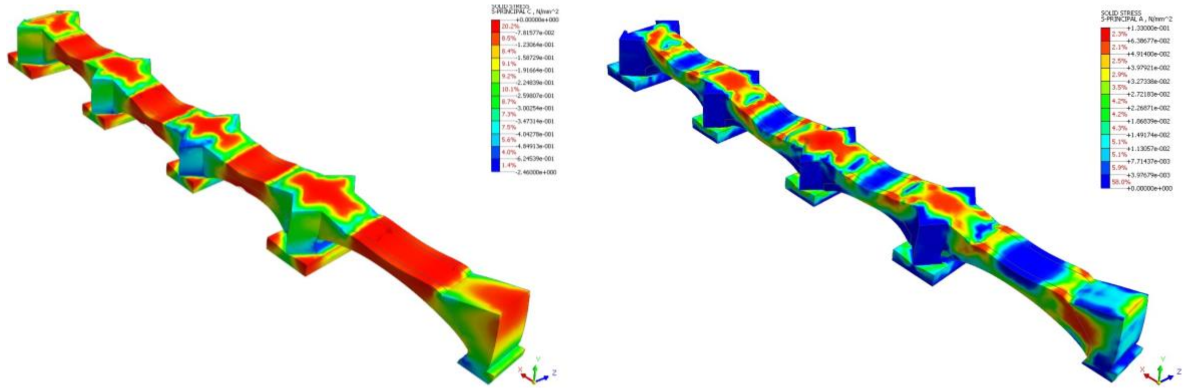

(d) (e)

Figure 10 Results of the nonlinear analysis to maximize the load on pier 3: (a) vertical displacement at the final step of the analysis – load multiplier 2, (b) material status of the elements at the final step of the analysis - load multiplier 2, (c) capacity curve function of the load multiplier and total applied load, (d) compression principal stress passed the safety limit - load multiplier 1.4, (e) tension principal stress passed the safety limit - load multiplier 1.4, (e).

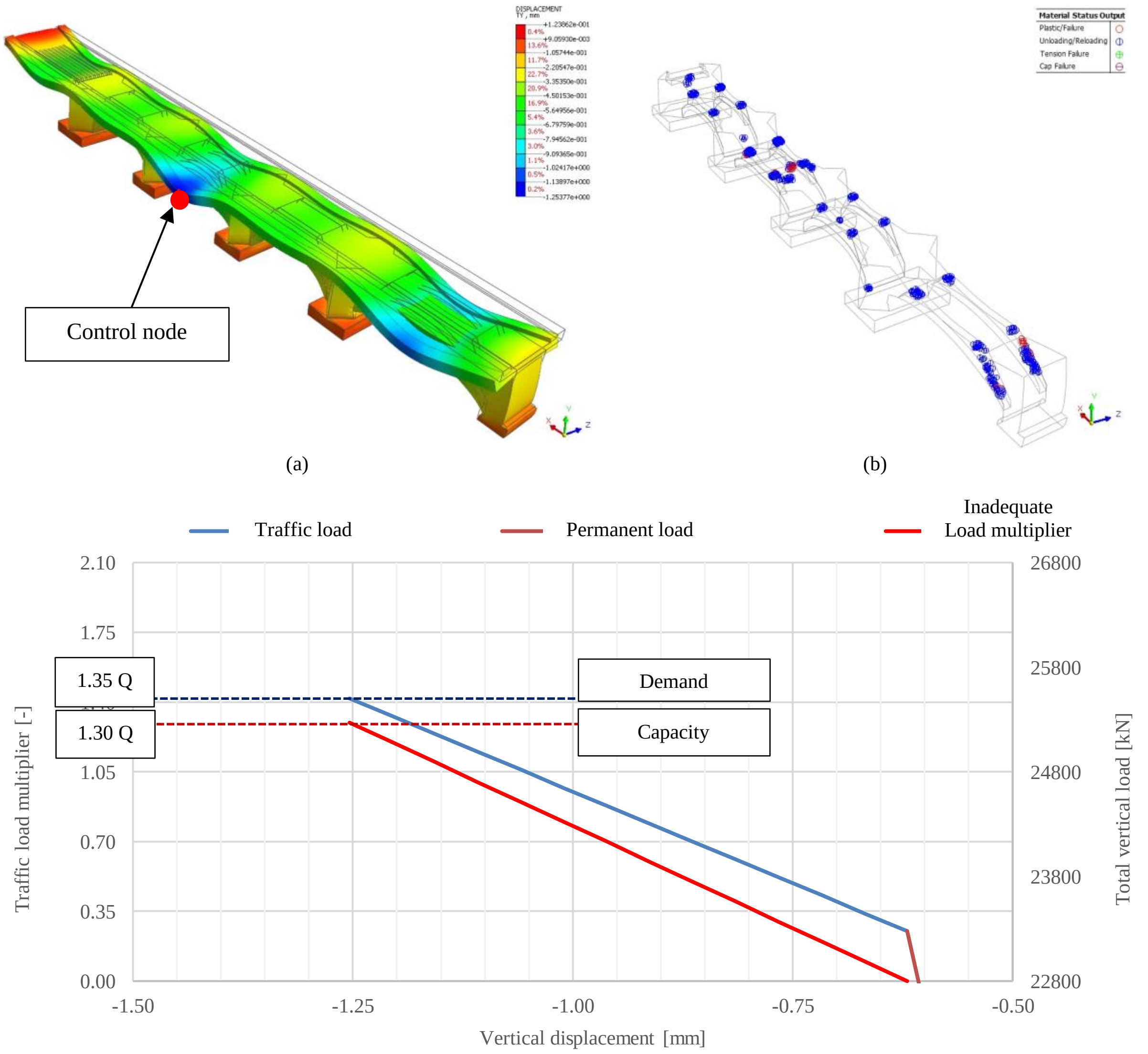

(a) (b)

(c)

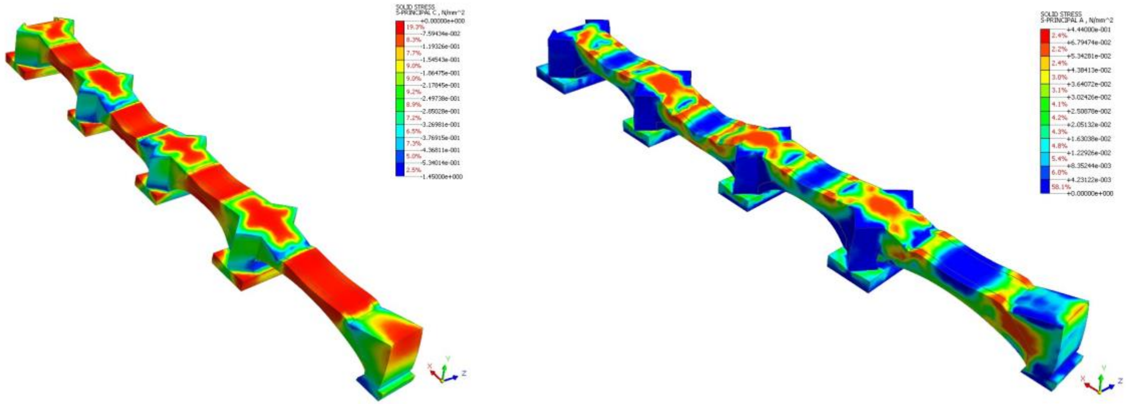

(d) (e)

Figure 11 Results of the nonlinear analysis to maximize the load on bay P2-P3: (a) vertical displacement at the final step of the analysis – load multiplier 1.3, (b) material status of the elements at the final step of the analysis - load multiplier 1.3, (c) capacity curve function of the load multiplier and total applied load, (d) compression principal stress at the final step of the analysis – load multiplier 1.3, (e) tension principal stress at the final step of the analysis – load multiplier 1.3, (e).

Two different control nodes were selected based on the largest vertical displacements (Figure 10a, Figure 11a). The capacity curves were represented in terms of total applied load and load multiplier of the characteristic vehicular load respect the vertical displacement of the control node, the plotted curves track the respond of the structure during vehicular traffic. Being both load and displacement in the vertical direction, the governing failure mechanism does not provide significant nonlinearity (Figure 10c, Figure 11c). In Figure 10b and Figure 11b is reported the material status which identities the element failure (in red) and stress change during cracking (in blue). The compression stress agrees with the material compressive strength (Figure 10d and Figure 11d), the tensile stress is larger than the tensile strength (uniaxial) since the state of triaxial stress provides confinement thus additional capacity (Figure 10e and Figure 11e). Load configuration in Figure 10 reaches maximum load multiplier 2, thus pier 3 is adequate to carry the prescribed traffic load. Load configuration in Figure 11 reaches maximum load multiplier 1.3 (below the limit value 1.35), thus bay P3-P2 is not adequate.

4 CONCLUSIONS

The work presents a comprehensive approach to assess the safety of masonry bridge that integrates recent technical advances as photogrammetric survey with UAV and the BIM working methodology, into established numerical analysis (as the nonlinear static analysis) applied to vehicular traffic.

The approach takes advantage of the benefits of the photogrammetric survey in the definition of the external geometry of the bridge and combines them with the information in the internal morphology present in the archival line drawing retrieved during the historical-critical analysis. The definition of an accurate, updated, and consistent geometry is rather important in the assessment of masonry structures.

The employment of nonlinear static analysis in the vertical direction resulted effective in the structural assessment even if unusual because nonlinear static analysis (as pushover analysis) is generally oriented in the horizontal direction to model the earthquake action.

A limitation of the safety evaluation of the bridge is the inability to superimpose the effects of multiple loads (as wind, earthquake, or thermal effect) because of the nonlinearity of the analysis, thus an efficient assessment requires the preliminary evaluation of the effects of the most significative actions and the identification of the potential vulnerabilities.

5 REFERENCES

[1] M. Solla, J. C. Caamaño, B. Riveiro, and P. Arias, “A novel methodology for the structural assessment of stone arches based on geometric data by integration of photogrammetry and ground-penetrating radar,” *Eng. Struct.*, vol. 35, pp. 296–306, Feb. 2012, doi: 10.1016/j.engstruct.2011.11.004.

[2] N. Domede, A. Sellier, and T. Stablon, “Structural analysis of a multi-span railway masonry bridge combining in situ observations, laboratory tests and damage modelling,” *Eng. Struct.*, vol. 56, pp. 837–849, Nov. 2013, doi: 10.1016/j.engstruct.2013.05.052.

[3] P. Borlenghi, A. Saisi, and C. Gentile, “ND testing and establishing models of a multi-span masonry arch bridge,” *J. Civ. Struct. Health Monit.*, Jan. 2023, doi: 10.1007/s13349-022-00666-1.

[4] Ministero delle Infrastrutture e dei Trasporti, *Norme tecniche per le costruzioni (NTC 2018) D. Min. Infrastrutture e Trasporti 17 gennaio 2018*. Legislazione tecnica, 2018.

[5] “Metashape Professional - Photogrammetry software v.1.5.2.” Agisoft LLC, St. Petersburg, Russia, 2020.

[6] “Revit 2021 -Software for the Building Information Modeling.” Autodesk, San Rafael, Oct. 13, 2021. [Online]. Available: www.autodesk.com/

[7] “Midas FEA NX.” MIDAS Information Technology Co., 2021.

[8] Ministero delle Infrastrutture e dei Trasporti, *Istruzioni per l’applicazione dell’«Aggiornamento delle “Norme tecniche per le costruzioni”» di cui al decreto ministeriale 17 gennaio 2018.* 2019.

[9] P. B. Lourenço and A. Gaetani, *Finite Element Analysis for Building Assessment: Advanced Use and Practical Recommendations*. Taylor & Francis, 2022.